Mechanisms of the Aqueous Solvolysis of the Ring-Opening of the Lactone Ring of Goniodomin A

ABSTRACT

The phycotoxin Goniodomin A is a Dinoflagellate of the Alexandrium genus and is a macrocyclic lactone. It is found widely in sea water and is known to break the lactone connection slowly in water. The cleavage of the lactone is sensitive to the pH of the water as one changes the pH from ~6 to 8 with the solvolytic rate of cleavage dramatically increasing. Treatment of kinetic data previously published indicates that there are likely two competing first-order reactions, an S_N1 and an intramolecular S_N2, pseudo first order reaction.

Key word : marine phytotoxin, mechanism of lactone hydrolysis, lactone epoxide ,carbocation, nucleophilic reactions

1. INTRODUCTION

The phycotoxin Goniodomin A (GDA,**1**) is a Dinoflagellate of the Alexandrium genus. GDA is produced by four species of the genus - *hiranoi*, *A. pseudogonyaulax*, *A. monilatum* and *A. taylorii*. [1] [2] [3] [4] While Morakami and Takeda determined the structure of GDA [1] [5] and its structure was recently confirmed by X-ray crystallography. [6] GDA is a polyketide macrolide containing six oxygen heterocycles, five macrocyclic rings with two of the five constituting spiro ketals. The sixth ring contains a hemiketal, which will be the focus in this manuscript.

In 2020 Onofrio reported that GDA degrades in pure water, presumably at pH 7 and significantly faster in sea water where the pH is approximately 8. [7] Further studies by Hintze [8] found that the rate of degradation of **1** in deionized water (~pH 6.5), MilliQ -Q water (pH 7.2) and in culture medium (pH 8.2) became

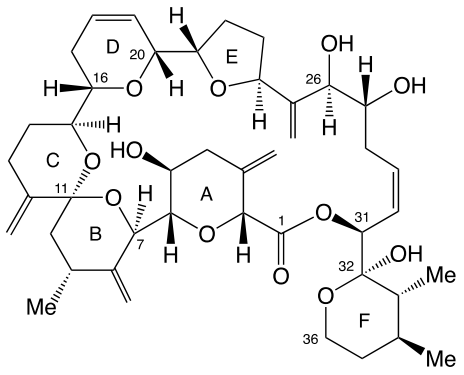

Chemical Structure 1: GDA (**1**)

significantly faster with increase of the pH. The product of the degradation is known to be a carboxylic acid such as the seco acid of GDA (**2**). At first blush one might expect the reaction to proceed with

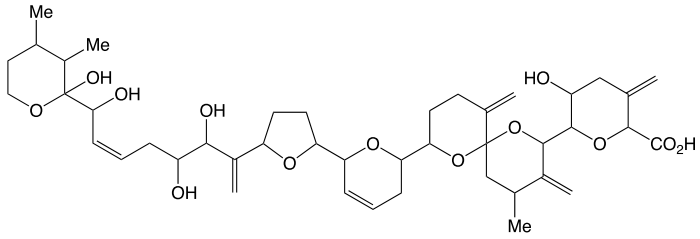

Chemical Structure 2: GDA-SA (**2**)

simply hydrolysis of the lactone. However, an alternative mechanism would be that of solvolysis with the leaving group being the carboxylate anion with production of a carbocation at C_{31}. While the carboxylate is one of the worst known leaving groups in nucleophilic substitutions, there are two aspects the structure of **1**, which might make the solvolytic mechanism the preferred one. The first is that the forming carbocation is allylic since the developing positive charge on C_{31} is allylic. The second one is the OH group at C_{32} might interact as a neighboring group in which case an epoxide would be formed or possibly the epoxide might simply exist on the pathway of a concerted reaction. In the latter case it would not form the C_{31} carbocation but rather the C_{32} carbocation, which would be stabilized by the ether oxygen lone pair. The solvolytic degradation of **1** was confirmed by Harris with $H_2{}^{18}O$. [9]

The purpose of this study is to treat computationally a model system to determine the solvolytic mechanism. The rather dramatic change in rate vs pH found by Hintze[8] suggests that there might be two competing mechanisms

2. KINETICS OF THE SOVOLYTIC REACTIONS

As mentioned above, Hintze studied the degradation of **1** at three different pH values. Included in his thesis were the plots of his kinetic data (concentration vs. time in days). It was found that these kinetic data all arose from first order reactions – straight lines were found when plotting the natural log of the concentration at time t divided by the initial concentration (t=0). Our kinetic treatment of these data are presented in Fig. 1.

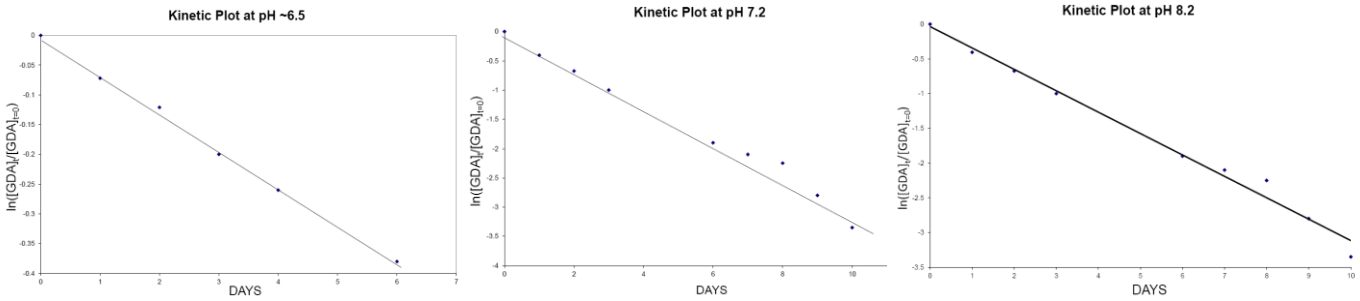

Fig. 1. **The kinetically treated data of Hintze at three different pH**

The $t_{1/2}$ half-lives of these three kinetic treatments are 3.4, 2.0 and 1.2 days, respectively. The dramatic change in $t_{1/2}$ lives suggests that there might be two competing first order reactions occuring, one being dominant at pH 6 and the other at pH 8. What is different at these two pH values? Given that it is likely that both are nucleophilic substitutions, it is possible that the hydroxide ion might be involved in the major reaction occurring at pH 8, since the hydroxide concentration is two orders of magnitude higher at pH 8 than at pH 6. At this point it was possible that the dominant reaction at pH 6 is S_N1 and at pH 8 S_N2. The calculations described below were done to confirm this proposal.

3. DFT CALCULATIONS.

The calculations [10] described below were done to explain the proposal based on the kinetic results. At pH 6 most likely an S_N1 reaction occurs with a unimolecular ionization with the carboxylate acting as the leaving group. Using the model system mentioned above a transition structure (4) was located, which suggested a concerted rearrangement with the forming carbocation (Fig. 2). As seen the ionization is assisted by the

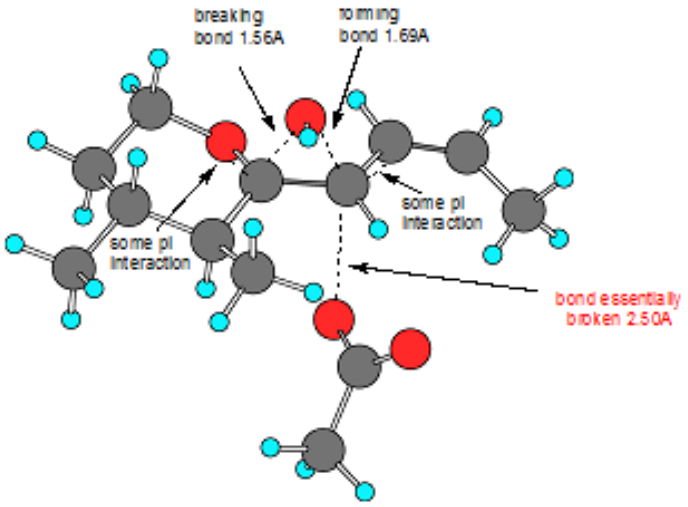

Fig. 2. The concerted, but asynchronous, transition structure for the S_N1 reaction dominant at pH 6

double bond attached to C_{31} as well as migration of the OH group from C_{32} to C_{31} and is further stabilized by interaction of the hemiacetal oxygen attached to C_{32}, which is crucial in stabilizing the final rearranged carbocation. Intrinsic Reaction Coordinate (IRC) calculations produced the reactant and product as shown in Fig. 3. In the case of the reactant the IRC gave a conformer of the that in the x-ray structure. [6]

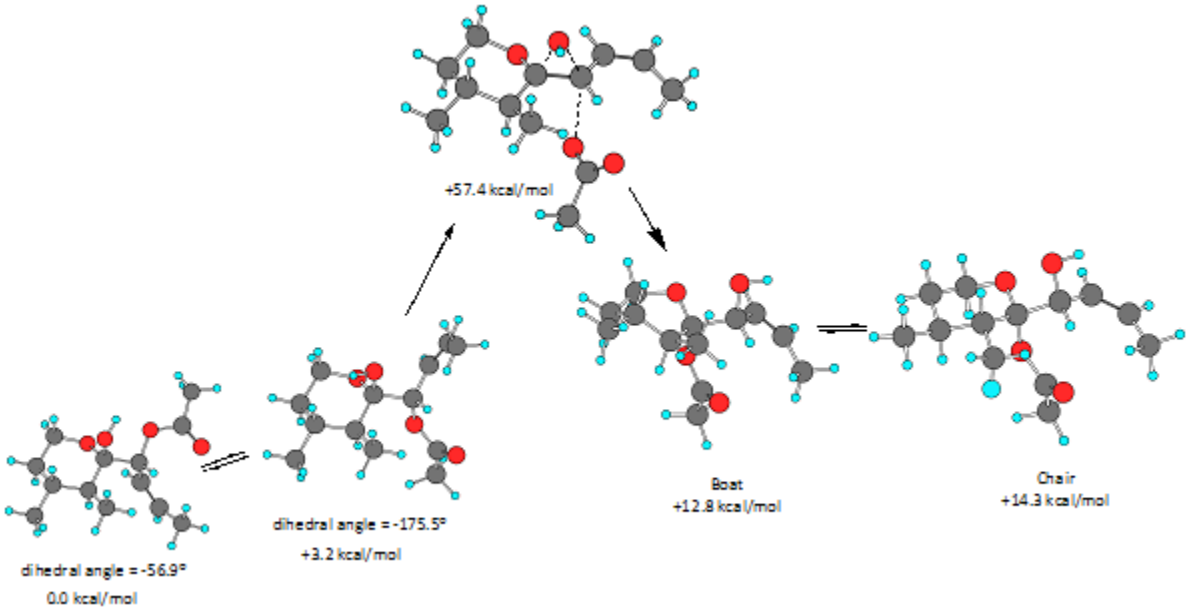

Fig. 3 The computed concerted reaction pathway for the S_N1 reaction dominant at pH 6

The IRC reactant conformer has a dihedral angle of the two carbons connecting the acyclic chain to the carboxylate carbon of the lactone of -175.5 and its conformer's dihedral angle is -56.9°. The x-ray conformer has a dihedral angle that would prevent OH group participation in the concerted reaction. The IRC gave a product with the six-membered ring in a boat conformation. Interestingly the chair conformer of the product was found to be higher in energy than that of the boat conformer.

While the DFT calculations were carried out in a water medium, S_N1 reactions are not properly described by these calculations [11], since it is known that it first forms a contact ion pair, which in turn forms a solvent separated ion pair. With this type of calculation, these ion pairs are not taken into account and the leaving group has only one choice, to collapse to the newly formed carbocation produced by the concerted reaction. The activation energy is also very large, since while the calculation is modeled with a surrounding solvent of water, no water molecules are present in the vicinity of the ionization of the C-O bond to "assist" in the ionization, such as the formation of the solvent separated ion pair. Consequently the computed activation energy is likely much higher than the experimental one.

However, it is possible to obtain a better estimate of the overall energetics of carbocation reactions by carrying out calculations on the carbocation which is formed. There is good evidence for this in recent computations of carbocation rearrangements in terpene chemistry. [12] Beginning with the carbocation that is formed by loss of the carboxylate group in our model system a transition structure (Fig. 5) was located very similar to that located above (Fig. 2).

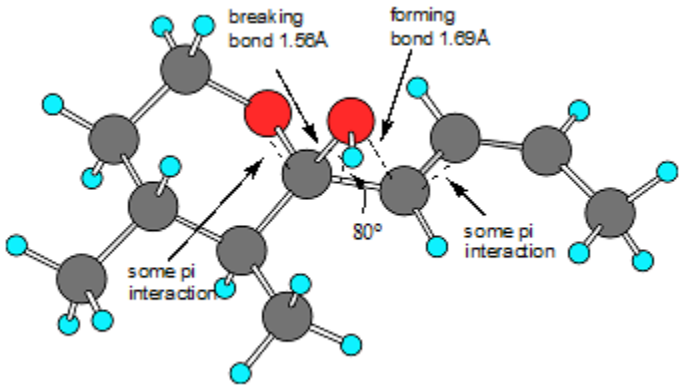

Fig. 4. The S_N1 transition structure (with an overall positive charge) located for the model system carbocation

Perhaps more dramatic is the difference in the overall energetics of the carbocation reaction (Fig. 5) than

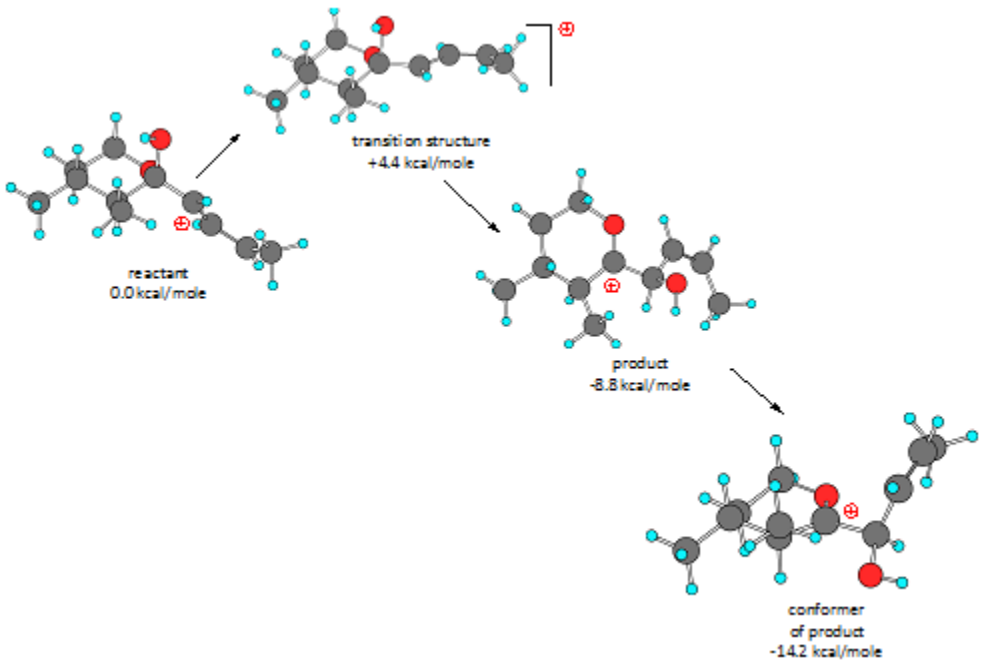

Fig. 5. The overall DFT pathway of the carbocation in the S_N1 reaction dominant at pH 6

that in Fig. 3. Note the very low activation energy (+4.0 kcal/mol) and the overall energy of reaction between the reactant and the IRC product of -14.5 kcal/mole. It is apparent that major driving force for this concerted rearrangement is the ability of the ether oxygen in the oxane ring to stabilize the carbocation on C_{32}. This is not unexpected given that the methoxy group has a large negative Hammett σ_{para} constant.

Turning to the dominant reaction at pH 8, a DFT study was conducted with the addition of a hydroxide ion. A transition structure was located (Fig. 6) for the removal of the hydrogen on the OH group on C_{32}.

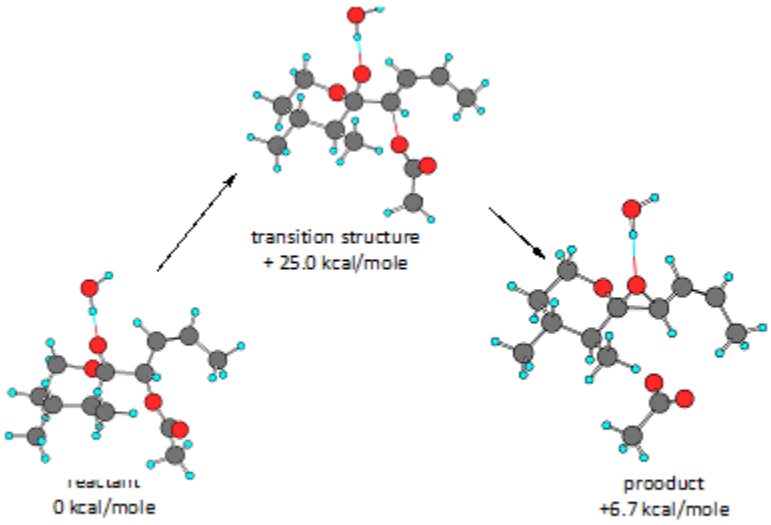

Fig. 6. The reaction pathway which includes a hydroxide ion of the solvolysis of the ester at pH 8 or under basic conditions

Again, the overall reaction studied in the modeled water solution suffers from no individual water molecules present in the vicinity of the structures along the reaction pathway. For example, the carboxylate leaving group would be hydrated with water molecules, which would of course likely change the overall energetics of the reaction. The pathway was also studied beginning with the anion of the reactant (Fig. 7). It is seen that

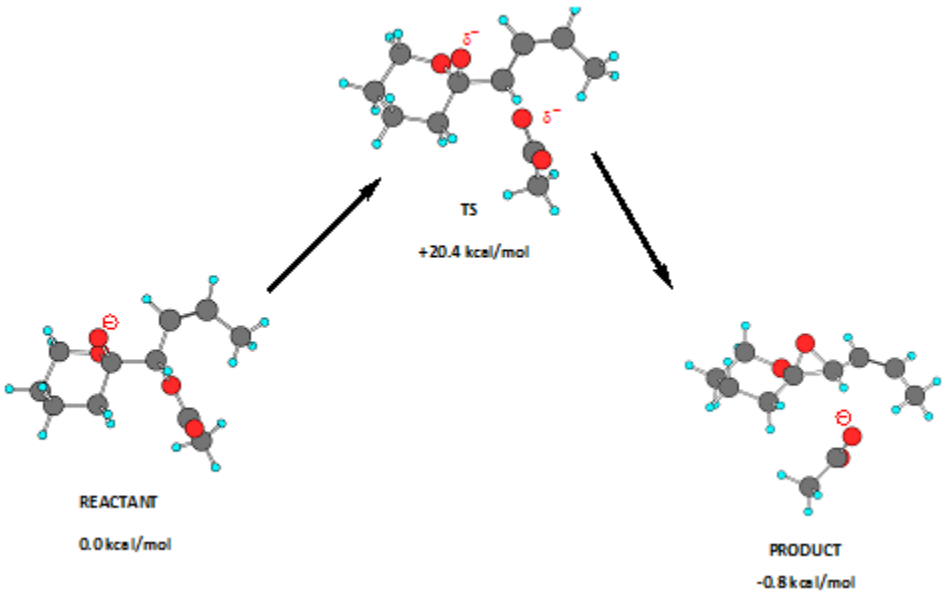

Fig. 7. The S_N2 reaction at pH 8 beginning with the proton removed from the oxygen at C_{32}

this reaction is indeed an intramolecular S_N2 reaction. In this case the attacking nucleus is the negatively charged oxygen on C_{32}. While the overall reaction energy is now negative, it is rather small at -0.8 kcal/mol. Again, these energetics are different from what one would expect experimentally because of lack of water molecules interacting with the structures along the reaction pathway.

Discussion

The study revealed that treatment of the kinetic data shown in Figure1, a dramatic increase in $t_{1/2}$ as pH is increased, is very likely a result of two competing first order reactions, both of which have a dependence on pH. At the lower pH the reaction is a typical S_N1 reaction with a neighboring group participation of the OH group on the carbon adjacent to the developing positive charge that is produced by the leaving group, the driving force being the formation of the positive charge on the adjacent carbon (Figure 5), which is stabilized by the oxane oxygen by participation of its unshared pair of electrons.

At higher pH the second reaction becomes dominant because of the increase in hydroxide ion concentration, which acting as a base removes the proton from the OH (see Figure 6) allowing the formation of the epoxide. In this reaction the rate determining step involves two reactants. Note that one of the reactants is the hydroxide ion and whose concentration is constant during the course of the reaction. Hence this is simply a pseudo first order reaction since the *change* in the concentration of the substrate is far more than that of the hydroxide. Hence the kinetic treatment shows two competing first order reactions, but as seen from the calculations the one at higher pH is in fact a pseudo first order reaction.

Whether or not the epoxide is stable or not under the basic reaction conditions is an interesting question. It has two pathways that ring opening of the epoxide can occur as shown in Fig. 8, with the two products being diastereomers and the product giving rise to the *R*-*R* one favored because of steric hindrance at the carbon undergoing the nucleophilic attack. Interestingly the S_N1 reaction would also give rise to a C_{31} *S* -C_{32} *S* glycol.

However under the aqueous conditions the C_{32} carbon might very well be racemized by mutarotation of the hemiketal.

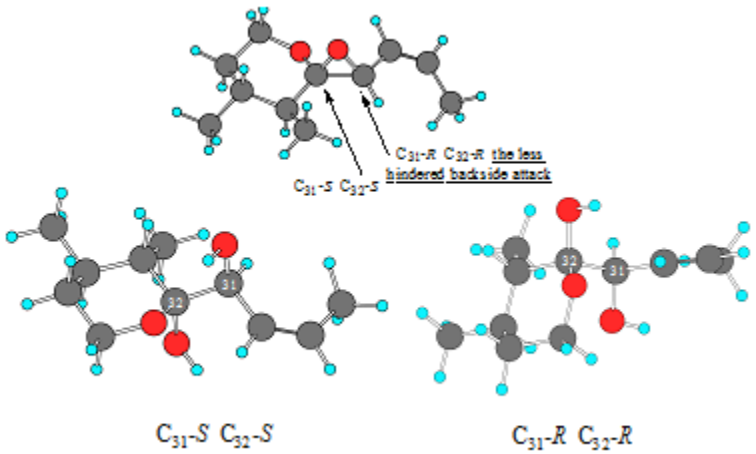

Fig. 8. Potential products of base catalyzed opening of the epoxide

4. CONCLUSIONS

The DFT results suggest that indeed there might be competing first-order nucleophilic substitution reactions. At the lower pH the S_N1 dominates and at higher pH an intramolecular S_N2 reaction is predicted to dominate as a pseudo first order reaction.

1. Murakami M, Makabe M, Yamaguchi K, Konosu S, Ichli W. Goniodomin a, a novel polyether macrolide from the dinoflagellate *goniodoma pseudogoniaulax.* Tetrahedron Lett. 1998; 29; 114-52.
2. Hsia MH, Morton SL, Smith LL, K. R. Beacuchesne KR, Huncik KM, Moeller PDR. Production of goniodomin A by the planktonic, chain-forming dinoflagellate Alexandrium monilatum (Howell) Balech isolated from the Gulf Coast of the United States Harmful Algae. 2006; (5); 290-9.
3. Triki HZ, Laabir P. Moeller N. Chomerat P, Daly-Yahia OK. First report of goniodomin A production by the dinoflagellate Alexandrium pseudogonyaulax developing in southern Mediterranean (Bizerte Lagoon, Tunisia) Toxicon, 2016; 111; 91-9.
4. Mertens KN, Adachi M, Anderson DM, Band-Schmidt CH, Bravo I, et al. Morphological and phylogenetic data do not support the split of Alexandrium into four genera. Harmful Algae 2020; 98**;** 101902.

5. Takeda Y J. Shim J, Oikawa M, Sasaki M. Assignment of the absolute configuration of goniodomin A by NMR spectroscopy and synthesis of model compounds. Org. Lett. 2008; 10; (5); 1013–6.
6. Tainter CJ, Schley ND, Harris CM, Stec DF, Song AK, Balinski A, et al. Algal toxin goniodomin A binds potassium ion selectively to yield a conformationally altered complex with potential biological consequences. J. Nat. Prod. 2020; 83; 1069-81.
7. Onofrio MD, Mallet CR, Place AR, Smith JL. A screening tool for the direct analysis of marine and freshwater phycotoxins in organic SPATT extracts from the Chesapeake Bay. Toxins. 2020; 12; 322-38.
8. Hintze L, Master Thesis. University of Applied Sciences. Mannheim. 2021.
9. Harris TM private communication.
10. All calculations were performed with Gaussian 09 (RevisionA.02). Frisch Trucks GW; Schlegel HB; Scuseria GE, Robb MA; Cheeseman JR, et al. Gaussian Inc. Wallingford CT 2009; Geometries were optimized without symmetry constraints using M06-2X/6-31G*. Wang Y, Verma O, Jin X, Truhlar DG. Revised M06 density functional for main-group and transition-metal chemistry. Proc. Natl. Acad. Sci. U. S .A. 2018; 115; 10257-62. Zhao Y, Truhlar DG. Theor. Cheim. Acta. 2008;120; 21542. Haraharan PC, Pople JA. The influence of polarization functions on molecular orbital hydrogenation energies. Theor. Chim. Acta. 1973; 28 213-222. All structures were characterized by frequency calculations and reported energies include zero-point energy corrections (unscaled). Intrinsic reaction coordinate (IRC) calculations. Gonzalez C, Schlegel HB. Reaction path following in mass-weighted internal coordinates. J. Phys. Chem. 1990; 94; 5523 –27. Frequency calculations were also used to characterize transition Structures. Fukui, K. The path of chemical reactions-the IRC approach. Acc. Chem. Res. 1981; 14; 363 – 8) were also used to verify the identity of all transition structures.
11. Otomo H, Suzuki R, Lida T, Takayanagi T. S_N1 reaction mechanisms of *tert*-butyl chloride in aqueous solution: What can be learned from reaction path search calculations and trajectory calculations for small hydrated clusters? Comp Theor. Chem. 2021; 1201; 113278-85.
12. (a) Smentek L, Hess Jr. B. A. Compelling computational evidence for the concerted cyclization of the ABC rings of hopene from protonated squalene. J. Am. Chem. Soc. 2010; 132; 17111-7; (b) Hess Jr. B. A, Smentek L. The Concerted Nature of the Cyclization of Squalene Oxide to the Protosterol Cation. Angew. Chem. Int. Ed. 2013; 52; 11029-33. (c) N. Chen S. Wang L. Smentek B. A. Hess Jr. R. Wu. *Angew. Chem. Int. Ed.* 2013 54 8693-8696; (d) Matsuda SPT, Wilson WK, Xiong Q. Mechanistic insights into triterpene synthesis from quantum mechanical calculations. Detection of systematic errors in B3LYP cyclization energies. Org. Biomol. Chem. 2006; (4) 530-543; (e) Tantillo TJ. Biosynthesis *via* carbocations: Theoretical studies on terpene formation. Nat. Prod. Rep. 2011; 28; 1035-53; (f) Hong YJ, Tantillo TJ. Which Is More Likely in Trichodiene Biosynthesis: Hydride or Proton Transfer? Org. Lett. 2006; 8; 4601-4; (g) Hong YJ, Tantillo TJ. Consequences of Conformational Preorganization in Sesquiterpene Biosynthesis: Theoretical Studies on the Formation of the Bisabolene, Curcumene, Acoradiene, Zizaene, Cedrene, Duprezianene, and Sesquithuriferol Sesquiterpenes. J. Am. Chem. Soc. 2009; 131; 7999-8015.